

Thermomechanical Behaviour of Mullite–Zirconia Composite

M. Hamidouche,^a N. Bouaouadja,^a H. Osmani,^a R. Torrecillas^b & G. Fantozzi^b

^aLaboratoire des Matériaux, IOMP Université de Sétif, Sétif 19000, Algeria

^bLaboratoire GEMPPM, UA 341, INSA de Lyon, France

(Received 24 January 1994; revised version received 26 March 1995; accepted 9 June 1995)

Abstract

Mullite is one of the most widely used compounds in many industrial products. It has been shown that addition of zirconia to mullite improves its mechanical properties, particularly at high temperature. Some investigations have been attempted to explain the fracture toughening of this material. In this paper, the mechanical properties of mullite–zirconia composite have been determined from room temperature up to 1400°C. The thermomechanical behaviour of this material is sensitive to the phase transformation of zirconia. The obtained results are presented and discussed.

1 Introduction

It is generally accepted that mullite (MAl_2O_3 – $NSiO_2$ with M/N ratio varying from 3:2 to 2:1) is one of the most widely encountered and important compounds found in many industrial ceramic products.^{1,2} However, mullite is difficult to consolidate into fully dense single-phase bodies. To optimize its mechanical properties, some investigations have been attempted using different processing techniques such as hot-pressing, hot-isostatic pressing and sol-gel processing.^{3,4}

Claussen and Jahn⁴ showed that significant toughening could be obtained by incorporating zirconia particles (ZrO_2) in a mullite matrix. Different mechanisms are involved in the toughening of mullite composite with zirconia additions: stress-induced transformation, microcracking, crack bowing and crack deflection.⁵ In all cases, the operative toughening mechanism depends on such variables as matrix stiffness, zirconia particle size, chemical composition, temperature and strength.

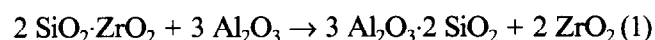
There are three main processing routes for producing mullite–zirconia composites,⁶ each leading to a special microstructure and then to specific properties. Mullite–zirconia material can be pro-

duced by conventional sintering of mechanical mixtures of fused mullite or reactive pre-mullite and zirconia powders. It can also be produced by an *in situ* reaction process between zircon ($ZrSiO_4$) and alumina to form mullite with dispersed zirconia. The third technique is based on sintering the mullite precursors (SiO_2 and Al_2O_3) with different zirconia contents.

The aim of this work is to determine the mechanical properties of a mullite–zirconia composite from ambient temperature up to 1400°C. Fracture toughness, fracture strength, elastic modulus and thermal shock are characterized and discussed in terms of the effect of zirconia at high temperature.

2 Experimental Procedure

The following compounds were used as starting materials: zircon fine powder (Ceraten SA, Spain) with 1 μm average particle size, and α -alumina powder (CT 3000 SG; Aleoa, Germany) with 0.5 μm mean particle size. Zircon and alumina are formed according to the following reaction:



The powder mixtures were ball-milled for 2 h using alumina balls and containers with isopropyl alcohol as milling medium. After evaporation of the liquid, the powder was cold-isostatically pressed at 200 MPa. The mullite–zirconia blocks were treated at 1600°C for 4 h. From these blocks, bars with dimensions $40 \times 6 \times 4$ mm³ were sawn for mechanical tests. The tensile surface was polished using a slurry containing 1 μm diamond grains.

Flexural strength measurements were made on samples of rectangular section (6×4 mm²) using four-point bending tests (inter/outer span: 10/35). The tests were carried out in air, from ambient temperature up to 1400°C, using an Instron testing machine equipped with a high temperature

furnace. The crosshead speed was 0.1 mm min^{-1} . Fracture toughness (K_{Ic}) was determined using single-edge notched beam (SENB) samples, tested in a three-point bending test. The ratio of notch depth to specimen width (a/W) was ~ 0.4 for all samples. The effect of crosshead speed on fracture toughness was observed using speeds of 0.2, 0.05 and $0.005 \text{ mm min}^{-1}$.

Thermal shock resistance was determined by flexural strength measurements after quenching in water (20°C) from different temperatures. The dilatometric curve has also been determined.

3 Results and Discussion

3.1 Chemical composition and phases

The bars were annealed for 12 h at 1200°C . Chemical composition (Table 1) was determined at room temperature by spectral analysis made with the 'Tracor' analyser of the Jeol scanning electron microscope (SEM).

Microscopic observation of the mullite-zirconia composite reveals a complex microstructure which contains three phases: mullite, zirconia and zircon (Fig. 1). The mullite grains are formed from agglomerates of about $10 \mu\text{m}$ size. Two types of zirconia grain are observed: spherical grains of $1 \mu\text{m}$ mean particle size which are located in the triple points, and rounded grains of about $3 \mu\text{m}$ mean grain size which are located normally in contact with zircon grains. Zircon grains are also present in the microstructure. The degree of dissociation

Table 1. Chemical composition obtained by spectral analysis for mullite-zirconia

	Al_2O_3	SiO_2	ZrO_2
Composition (wt%)	42.40	16.00	41.46



Fig. 1. Microphotographs of the structure of mullite-zirconia showing the scattering of zirconia particles.

of zircon is strongly dependent on the alumina fraction present in the initial mixture. Reaction sintering in the $\text{ZrSiO}_4\text{-Al}_2\text{O}_3$ system proceeds by atomic solution-diffusion-reprecipitation.⁷ The SiO_2 phase, which is always present on the zircon grains, primarily forms a residual glass phase situated in the grains boundaries of ZrSiO_4 and at zirconia-mullite interfaces, but not at mullite-mullite grain boundaries. This distribution most likely results from interfacial energy differences. The heat-treated sample exhibits a fractional content of 0.2 tetragonal and 0.8 monoclinic zirconia. The rounded appearance of the zirconia particles results from thermal etching, as revealed on fracture surfaces where the particles have the normal faceted morphology. The addition of zirconia promotes densification and retards grain growth. Compared with bodies produced by natural sintering of mixtures of mullite and zirconia powders,³ our materials present a higher amorphous phase for a corresponding zirconia volume fraction. This difference can be understood on the basis of the microstructural formation. It is evident that at high temperature, the strength of this material is affected by the viscosity of the glassy phase.

3.2 Mechanical behaviour

The mechanical characteristics of the studied material (fracture strength R , elastic modulus E , fracture toughness K_{Ic} , thermal shock resistance ΔT_c and linear expansion coefficient α) determined at room temperature are listed in Table 2. The effect of crosshead speed (s) on K_{Ic} values at room temperature is presented in Table 3. Thermal shock resistance is determined by the critical quenching temperature ΔT_c which leads to severe cracking of the composite, and then to low

Table 2. Mechanical characteristics obtained at room temperature ($T = 20^\circ\text{C}$) for mullite-zirconia composite

σ_f (MPa)	E (GPa)	K_{Ic} ($\text{MPa m}^{1/2}$)	ΔT_c ($^\circ\text{C}$)	$\alpha \times 10^6$ ($^\circ\text{C}^{-1}$)
215	150	4.2	300	1.62

Table 3. K_{Ic} values obtained at high temperature with three different crosshead speeds

$T(^\circ\text{C})$	$s \text{ (mm min}^{-1}\text{)}$		
	0.2	0.05	0.005
20	4.2 ± 0.3	4.0 ± 0.3	3.2 ± 0.4
800	3.6 ± 0.3	4.1 ± 0.4	2.9 ± 0.2
900	3.8 ± 0.2	4.2 ± 0.3	3.1 ± 0.2
1000	3.5 ± 0.5	3.8 ± 0.4	3.1 ± 0.3
1100	3.9 ± 0.2	4.0 ± 0.1	3.0 ± 0.1
1200	3.5 ± 0.1	3.0 ± 0.3	2.5 ± 0.3
1300	2.2 ± 0.3	2.8 ± 0.2	—

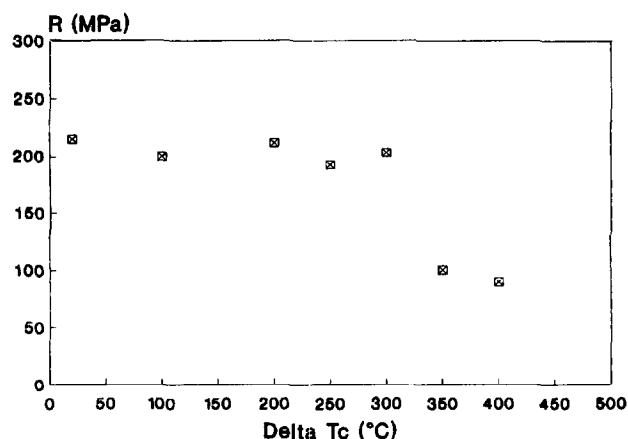


Fig. 2. Thermal shock curve of mullite-zirconia.

strength values. The obtained behaviour is plotted in Fig. 2. This mullite-zirconia composite shows better thermal shock resistance than pure mullite.⁸ The strength, after thermal shock, increased considerably in systems containing additions from 10 to 20 vol% of ZrO₂.

3.2.1 Dilatometric behaviour

To study the dilatometric behaviour, a test was carried out from ambient temperature up to 1400°C. Figure 3 shows the thermal expansion curve of a rectangular mullite-zirconia specimen (10 × 5 × 4 mm³), which exhibits an average linear expansion of $1.6 \times 10^{-6} \text{ } ^\circ\text{C}^{-1}$ with temperatures up to 1100°C. The hysteresis exhibited during this test indicates that there is a zirconia phase transformation. These results contrast with the data of Ruh *et al.*,⁹ who did not observe the transformation in mullite with 35% ZrO₂ and 1.5% Y₂O₃. This is reasonable because our samples present a great amount of monoclinic phase (~80%). The curve shows a phase transformation corresponding to a zirconia compound. This phase transformation occurs at 1100°C during heating (monoclinic → tetragonal) and at 785°C during cooling (tetragonal → monoclinic).

3.2.2 Flexural strength

Fracture strength values, established at different temperatures up to 1400°C, are plotted in Fig. 4. At room temperature our mullite-zirconia pre-

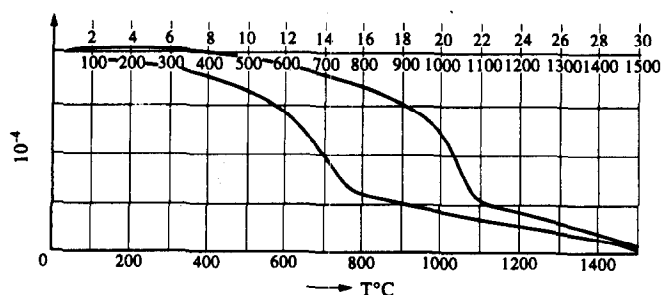


Fig. 3. Dilatometric curve of mullite-zirconia.

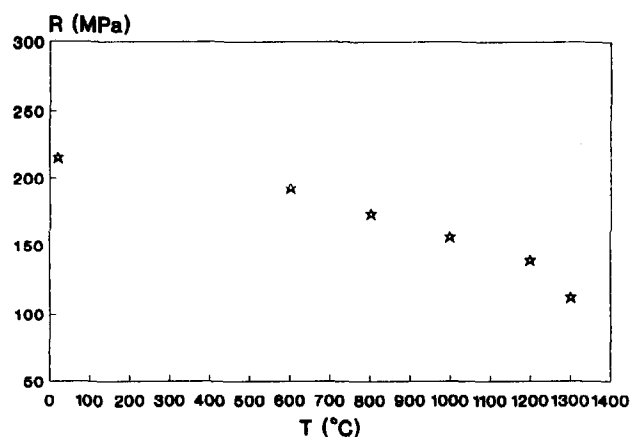


Fig. 4. Variation of fracture strength versus temperature.

sents a fracture strength of about 215 MPa, which is half the value found by Claussen and Jahn⁴ for a mullite-zirconia elaborated by reaction sintering and having approximately the same zirconia content. This wide difference can be explained by the differences in density (3.71 g cm^{-3} in our case, compared with 3.76 g cm^{-3}) and grain sizes of the mullite matrix and zirconia which are more than twice Claussen and Jahn's values (10 and $3 \text{ } \mu\text{m}$ respectively in our case, compared with 4 and $1 \text{ } \mu\text{m}$). The sintering time was 4 h in our case instead of 1 h in Claussen and Jahn's study made at the same temperature, giving them smaller grain sizes of zirconia and mullite. The authors explain the good mullite-zirconia characteristics by the separation of the sintering and reaction steps,⁴ which has not been done in our case.

From room temperature to 1400°C there is a slow and continuous decrease of flexural strength. Up to 1200°C, the load-displacement curves exhibit linear behaviour with limited apparent plasticity. The flexural strength R at 1200°C is half its room temperature value. The amorphous phase is probably the cause of this decrease in R .

It has been demonstrated that corrosion at the crack tip results in the formation of a surface layer of amorphous SiO₂ and viscous flow of the grain-boundary glass phase, the driving force for which is minimization of the surface energy. A further increase of temperature decreases the viscosity of the glassy phase for this material, resulting in a loss in fracture strength.

3.2.3 Elastic modulus

Elastic modulus was determined using a static method from load-displacement curves (Fig. 5). At room temperature, E is about 150 GPa. This value is in good agreement with results reported by Qi-Ming *et al.*¹⁰ for a mullite-zirconia composite with 25 vol% ZrO₂ (average grain size of $1 \text{ } \mu\text{m}$). The variation of E with temperature seems regular

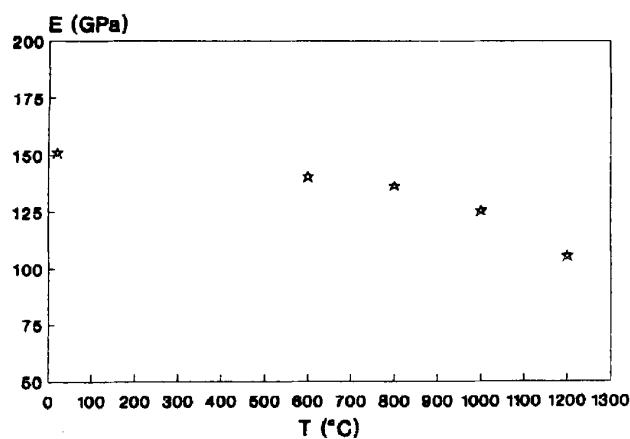


Fig. 5. Variation of Young's modulus versus temperature.

up to 900°C, beyond which there is a sensitive decrease of the curve. Elastic modulus reaches 105 GPa at 1050°C. As temperature increases, the stiffness of atomic linking decreases as a consequence of thermal agitation. The elastic modulus decrease is regular as far as the phenomenon is governed by these mechanisms. However, at a limit temperature value, intergranular phases become sufficiently viscous and generate sliding in the grain boundaries. Consequently, there is a sensitive decrease of elastic modulus.

3.2.4 Fracture toughness

The critical stress intensity factor is calculated using the equation:

$$K_{Ic} = \sigma_f Y \sqrt{a} \tag{2}$$

with

$$\sigma_f = 3 P_f L / 2 B W^2 \tag{3}$$

where *Y* is the geometric correction factor, *a* is the crack length, *P_f* is the maximum load, *L* is the span (three-point bending test), *B* and *W* are respectively the width and depth of the SENB samples.

The fracture toughness value (4.2 MPa m^{1/2})

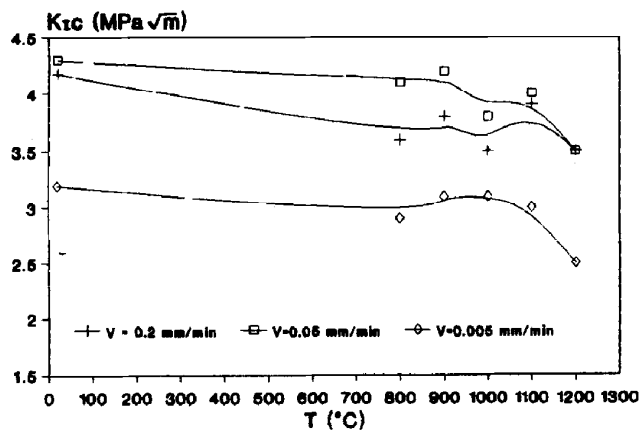


Fig. 6. Variation *K_{Ic}* versus temperature at three different crosshead speeds.

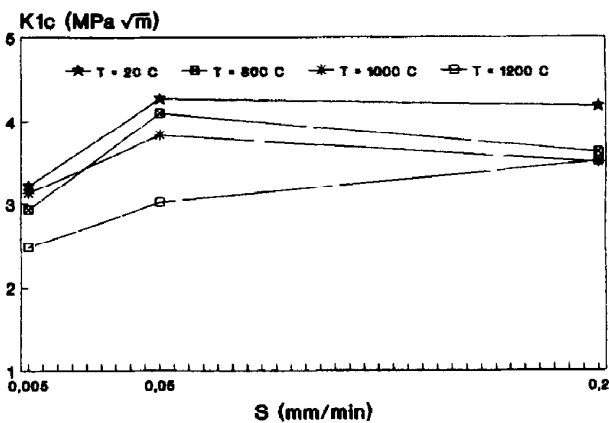


Fig. 7. Variation *K_{Ic}* versus crosshead speed at different temperatures.

found at room temperature is of the same order as values reported by Claussen and Jahn (4.5 MPa m^{1/2})⁴ and Ruh *et al.* (4.2 MPa m^{1/2}).⁹ The average *K_{Ic}* values established at high temperature with three different crosshead speeds are given in Table 3. The *K_{Ic}* versus temperature curves established at three different crosshead speeds, and the *K_{Ic}* versus crosshead speed *S* curves established at different temperatures, are shown in Figs 6 and 7, respectively.

When considering the fracture toughness values at room temperature and in the range 800–900°C it appears that the fracture mechanism is the same; i.e. fracture occurs by unstable crack extension from critical flaws. The fracture is typically transgranular (Fig. 8). *K_{Ic}* decreases linearly as the temperature increases according to the reduction of fracture energy. To determine which mechanisms are responsible for the toughness behaviour observed in this material, it is necessary to take into account the effects of the zirconia toughening and the microstructure.

In the case of mullite–zirconia composite, the monoclinic → tetragonal transformation occurs at about 1070°C. This phase modification explains

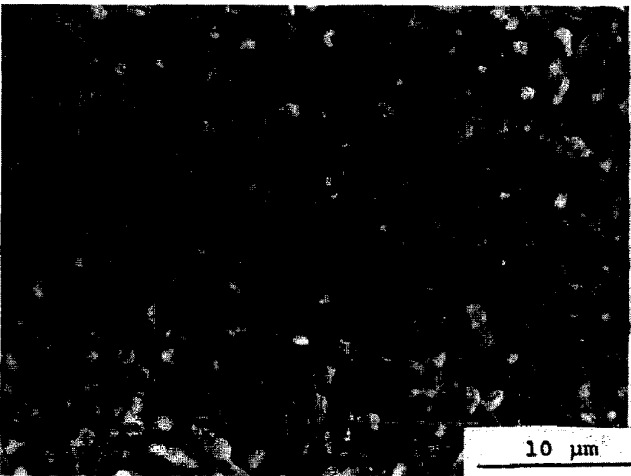


Fig. 8. Fracture facies showing transgranular cracks (*T* = 800°C).



Fig. 9. Fracture facies showing intergranular cracks ($T = 1100^{\circ}\text{C}$).

the observed decrease of K_{Ic} values. Above 900°C , the glassy phase becomes more fluid. Consequently, sliding in grain boundaries becomes more important than plastic relaxation and can lead to the formation of cracks and debonding of the matrix which, in turn, leads to a decrease of K_{Ic} values. In this domain of temperature, the load–displacement curves exhibit some plasticity and the fracture is typically intergranular (Fig. 9).

The mullite matrix presents mainly an intergranular fracture. The zirconia particles present three kinds of fracture mode: some show a single fracture plane, the largest and most irregularly shaped particles show several differently oriented cleavage planes and the largest round particles are surrounded by the crack. The same mechanisms have been observed in an other ceramic composite by Baudin *et al.*¹¹

3.2.5 Effect of crosshead loading speed on K_{Ic}

Crosshead speed is a parameter which has a sensitive effect on fracture toughness values (see Fig. 7). At low crosshead loading speed ($S = 0.005 \text{ mm min}^{-1}$), the low crack growth phenomenon prevails in the grain boundaries (reaction in crack front). This leads to crack increase and to low K_{Ic} values. At intermediate speed ($S = 0.05 \text{ mm min}^{-1}$), the material responds globally to the applied loading. The microstructure is strengthened because of the damage zone at the crack tip. On the other hand, upon a further increase in crosshead speed ($S = 0.2 \text{ mm min}^{-1}$), the phenomena described previously do not have sufficient time to grow. This leads to brittleness of the material.

4 Summary and Conclusions

- (1) Phase transformation of zirconia (monoclinic \rightarrow tetragonal) occurs at 1100°C during heating and at 785°C during cooling (tetragonal \rightarrow monoclinic).
- (2) The thermal shock resistance of mullite–zirconia is $\sim 300^{\circ}\text{C}$.
- (3) Young's modulus decreases linearly with temperature. It is 150 GPa at room temperature and 105 GPa at 1050°C .
- (4) At low temperature, the zirconia phase exhibits a positive effect on fracture strength.
- (5) At high temperature, phase transformation of the zirconia marked the fracture toughness decrease
- (6) The K_{Ic} maximum versus crosshead loading speed is shifted towards high temperature when crosshead speed increases.

References

1. Torrecillas, R., De Aza, S., Moya, J. S., Epicier, T. & Fantozzi, G., Improved high temperature mechanical properties of zirconia doped mullite. *J. Mater. Sci. Lett.*, **9** (1990) 1400–2.
2. Skoog, A. J. & Moore, R. E., Refractory of the past for the future: mullite and its use as a bonding phase. *Ceram. Bull.*, **67** [7] (1988) 1180–4.
3. Prochazka, S., Wallace, J. S. & Claussen, N., Microstructure of sintered mullite–zirconia composites. *Commun. J. Am. Ceram. Soc.*, (1983) C125–C127.
4. Claussen, N. & Jahn, J., Mechanical properties of sintered in situ-reacted mullite–zirconia composites. *J. Am. Ceram. Soc.*, **63** [3–4] 228–9.
5. Deportu, G. & Henney, J. W., The microstructure and mechanical properties of mullite–zirconia composites. *Brit. Ceram. Trans. J.*, **83** (1984) 69–72.
6. Orange, G., Fantozzi, G., Cambier, F., Leblud, C., Anceau, M. R. & Leriche, A., High temperature mechanical properties of reaction sintered mullite–zirconia composites and mullite–alumina–zirconia composites. *J. Mater. Sci.*, **20** (1985) 2533–40.
7. Di Rupo, E. & Anceau, M. R., Solid state reactions in the $\text{ZrO}_2\text{-SiO}_2\text{-}\alpha\text{-alumina}$ system. *J. Mater. Sci.*, **15** (1980) 114–8.
8. Hamidouche, M., Comportement thermomécanique de la mullite et de la mullite–zircon. Magister thesis, IOMP University of Sétif, 1992.
9. Ruh, R., Mazdiyasni, K. S. & Mendiratta, M. G., Mechanical and microstructural characterization of mullite and mullite–SiC whisker and ZrO_2 toughened-mullite–SiC whisker composites. *J. Am. Ceram. Soc.*, **71** [6] (1988) 503–12.
10. Qi-Ming, Y., Jia-Qi, T. & Zhen-Guo, J., Preparation and properties of zirconia-toughened mullite ceramics. *J. Am. Ceram. Soc.*, **69** [3] (1986) 265–7.
11. Baudin, C., Cambier, F. & Delaey, L., Fractographic and acoustic emission of mullite–alumina–zirconia composites prepared by reaction sintering. *J. Mater. Sci.*, **22** (1987) 4398–402.